AIP Applied Physics Letters

Nanopatterning of diarylethene films via selective dissolution of one photoisomer

Precious Cantu, Trisha L. Andrew, and Rajesh Menon

Citation: Applied Physics Letters **103**, 173112 (2013); doi: 10.1063/1.4826925
View online: http://dx.doi.org/10.1063/1.4826925
View Table of Contents: http://scitation.aip.org/content/aip/journal/apl/103/17?ver=pdfcov
Published by the AIP Publishing

Advertisement:

Goodfellow
metals • ceramics • polymers
composites • compounds • glasses
Save 5% • Buy online
70,000 products • Fast shipping

This article is copyrighted as indicated in the abstract. Reuse of AIP content is subject to the terms at: http://scitation.aip.org/termsconditions. Downloaded to IP: 128.104.69.234 On: Thu, 31 Oct 2013 14:50:38

Nanopatterning of diarylethene films via selective dissolution of one photoisomer

Precious Cantu,[1] Trisha L. Andrew,[2] and Rajesh Menon[1,a)]
[1]*Department of Electrical and Computer Engineering, University of Utah, Salt Lake City, Utah 84112, USA*
[2]*Department of Chemistry, University of Wisconsin-Madison, Madison, Wisconsin 53706, USA*

(Received 30 September 2013; accepted 11 October 2013; published online 24 October 2013)

The ability to pattern nanometric features on various substrates with high throughput, accuracy, and uniformity is the key driving force enabling novel applications in nanophotonics, nanoelectronics, nano-electro-mechanical systems, and nanofluidics. Patterning via Optical Saturable Transitions (POST) is an optical nanopatterning technique that circumvents the far-field diffraction limit by exploiting the linear switching properties of thermally stable photochromic molecules. Previously, POST was enabled by an electrochemical oxidation "locking step." In this letter, we report an electrode-free "locking step" that exploits the difference in solubility between the two isomeric states of a photochromic molecule in a polar solvent. The reported method obviates the need for a conducting underlayer and also reduces the number of required steps. Using this method, we demonstrated isolated lines of width $\sim\lambda/4$ and spacing between features as small as $\sim\lambda/2.5$ for an exposure wavelength of λ. *© 2013 Author(s). All article content, except where otherwise noted, is licensed under a Creative Commons Attribution 3.0 Unported License.* [http://dx.doi.org/10.1063/1.4826925]

Nanopatterning with optical wavelengths has many potential applications in the research, development, and manufacture of electronic, optical, and photonic devices.[1–4] Currently, geometries at the nanoscale are patterned primarily via serial writing tools such as scanning-electron-beam lithography, scanning-ion-beam lithography, and scanning-probe lithography. Although these tools offer high resolution and flexibility, their slow writing speeds prevent patterning of nanostructures over large areas. On the contrary, optical lithography can be extremely fast. However, its resolution is limited by diffraction.[5–7] Several techniques such as photo-induced deactivation (RAPID)[8] lithography, multiphoton absorption polymerization,[9] absorbance-modulation-optical lithography (AMOL),[10] and two-photon continous flow lithography (TP-CFL)[11] have been proposed to circumvent this far-field diffraction limit. The first two of these suffer from poor image contrast and require high light intensities, which limit their potential for parallelizability and high throughput. AMOL is limited to surface (2-D) patterning and in its current implementation also suffers from the requirement of high light intensities.[10] The last approach is not easily scalable to large volumes. Recently, we developed patterning via optical saturable transitions (POST) as an alternative technique for sub-diffraction-limited patterning.[5] POST exploits the photoisomerization at low light intensities of photochromic molecules, namely, diarylethenes, to create sub-diffraction-limited nanoscale patterns. Periodic features with sub-wavelength resolution have been reported before using other photochromic molecules,[12] namely, azobenzene polymers. However, the *cis* isomer of azobenzene is thermally unstable compared to the *trans* isomer and will spontaneously relax back to the *trans* form. This thermal isomerization reaction limits the subwavelength resolution limit achievable with azobenzene photochromes.[12] Diarylethenes have an advantage over azobenzenes as they are thermally stable at room temperature. Also, since only single-photon transitions are involved, POST does not have the restriction of high light intensity to achieve nanoscale resolution.

In POST, a thin layer of photochromic molecules acts as the pattern-recording material. The principle of operation is related to nanoscale fluorescence imaging where the samples are labeled with photoswitchable fluorophores such as in stimulated-emission-depletion microscopy (STED).[13,14] In STED, a focused round spot first excites the fluorophores in a diffraction-limited region. Subsequently, a focused ring-shaped spot at a longer wavelength de-excites the molecules through stimulated emission in this region except at the center of the ring. Only fluorophores in the center of the ring remain in the excited state and spontaneously emit photons. This light-emitting region can be substantially smaller than the far-field diffraction limit. The one key difference in nanopatterning is that a "locking" step is necessary to fix the sub-wavelength region and isolate it from further optical processing.[14] The specific sequence of steps for POST is described next.

In the POST process, a thin film of a photochromic molecule is first thermally evaporated onto a silicon substrate. In our experiments, the photochromic molecule is 1,2-bis(5,5′-dimethyl-2,2′-bithiophen-4-yl) perfluorocyclopent-1-ene (compound 1 in Fig. 1(a)). This layer is analogous to the pattern-recording material or the resist in conventional lithography. The layer is uniformly illuminated with a short-wavelength UV lamp (UVGL-25, Analytika Jena AG), which converts all molecules to the closed-ring isomer (compound 1c). Next, the sample is exposed to a standing wave at $\lambda_2 = 647$ nm (Kr-ion laser, Coherent Innova 301C). This exposure converts all molecules except at the nodes to the

a)Email: rmenon@eng.utah.edu

 © Author(s) 2013

This article is copyrighted as indicated in the abstract. Reuse of AIP content is subject to the terms at: http://scitation.aip.org/termsconditions. Downloaded to IP: 128.104.69.234 On: Thu, 31 Oct 2013 14:50:38

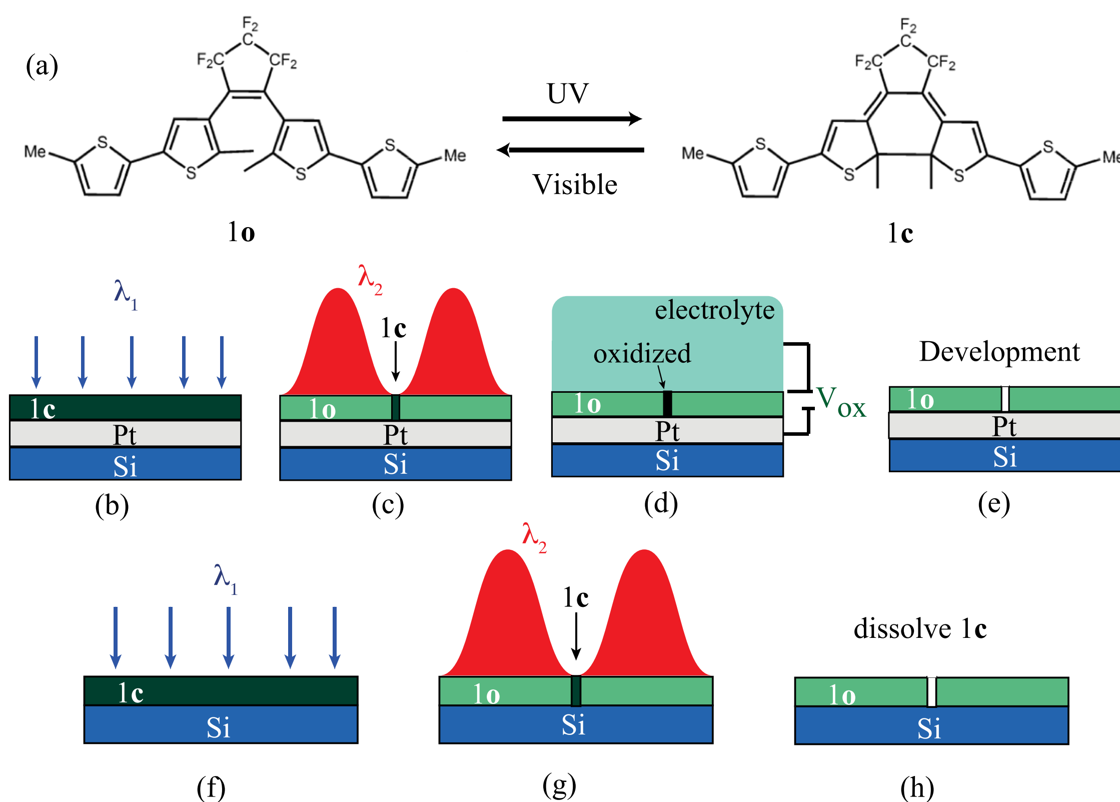

FIG. 1. (a) Photochromic molecule (compound 1) used as recording medium in POST. Compound 1 exists as an open-ring isomer 1o and a closed-ring isomer 1c. (b)–(e) Sequence of steps for conventional POST. (f)–(h) Sequence of steps for the new dissolution-based method.

open-ring isomer (compound 1o). Increasing this exposure time decreases the width of the regions that remain as 1c beyond the far-field diffraction limit. In conventional POST (Figs. 1(b)–1(e)), electrochemical oxidation selectively oxidizes 1c while 1o remains unchanged. The oxidized 1c is subsequently developed in a polar solvent mixture of 5%(wt.) isopropyl alcohol and 95%(wt.) ethylene glycol. We recently discovered that it is possible to selectively dissolve away 1c in 100%(wt.) ethylene glycol without affecting 1o. This step essentially achieves the "locking" of the pattern as illustrated in Figs. 1(f)–1(h). Note that this approach uses one less step than the conventional method. Furthermore, the conventional method requires a 100-nm-thick film of platinum underneath compound 1 to serve as the working electrode in a three-electrode electrochemical cell.[5,6] This, in turn, requires an additional evaporation step during sample preparation. Furthermore, it introduces challenges for pattern transfer into the underlying substrate after patterning. This approach reduces the number of required steps, is more general, and has the potential to be integrated into conventional optical-projection lithography, where water immersion is typically used.[15]

Compound 1o closes its central ring under UV irradiation, leading to a completely π-conjugated current path along the long axis of the molecule. Visible light irradiation of compound 1c opens the ring, breaking the conjugation length in half.[16] The central fluorocarbon tether acts as a through-space electron density-withdrawing group and introduces a dipole in both isomers of compound 1. The longer π-conjugation length, i.e., larger conjugated electron density, in the closed form leads to a larger dipole moment than for the broken π-system of the open form. This makes the closed-ring isomer 1c comparatively more polar and, therefore, more soluble in a polar solvent such as ethylene glycol.

To verify this selective solubility on the macro scale, we thermally evaporated a $\sim$22 nm thick layer of compound 1 at 100 °C and a base pressure of 1×10^{-6} Torr onto a clean silicon substrate and exposed half the sample to uniform illumination at $\lambda_2 = 647$ nm (CW Kr-ion, Coherent Innova 301C) for 10 min with an output laser power of $\sim$38 mW at an incident intensity of 2.15 mW/cm^2. This converts half the sample to 1o while the other half remains as 1c. The entire sample was then immersed in 100%(wt.) ethylene glycol for time intervals ranging from 5 min to 105 min, as illustrated in Fig. S2 of the supplementary material.[17] The remaining film thicknesses in both regions were measured with a Tencor P-10 profilometer after each immersion step. The results plotted in Fig. 2(a) confirm that while 1c is dissolved away, 1o remains mostly unaffected even after 105 min of immersion. The dissolution rate of 1c is 0.0565 nm/min while that of 1o is negligible. The ratio of the dissolution rate of 1c to that of 1o is higher than 20:1.[17]

Figure 2(b) shows the atomic-force micrographs of three grating patterns that were created in $\sim$29 nm-thick film of compound 1 atop a silicon substrate. Using a Lloyd's mirror interferometer, the samples were exposed to a standing wave of period 540 nm at $\lambda_2 = 647$ nm (incident intensity $= 2.1$ mW/cm^2) for 647 s. The samples were immersed in 100%(wt.) ethylene glycol for varying times. Subsequently, each sample was rinsed in deionized water and dried with N_2. From these two plots, one can clearly see the agreement of the dissolution rates of the closed-ring isomer 1c, in the macro-scale (Fig. 2(a)) with that at the nanoscale (Fig. 2(b)).

This article is copyrighted as indicated in the abstract. Reuse of AIP content is subject to the terms at: http://scitation.aip.org/termsconditions. Downloaded to IP: 128.104.69.234 On: Thu, 31 Oct 2013 14:50:38

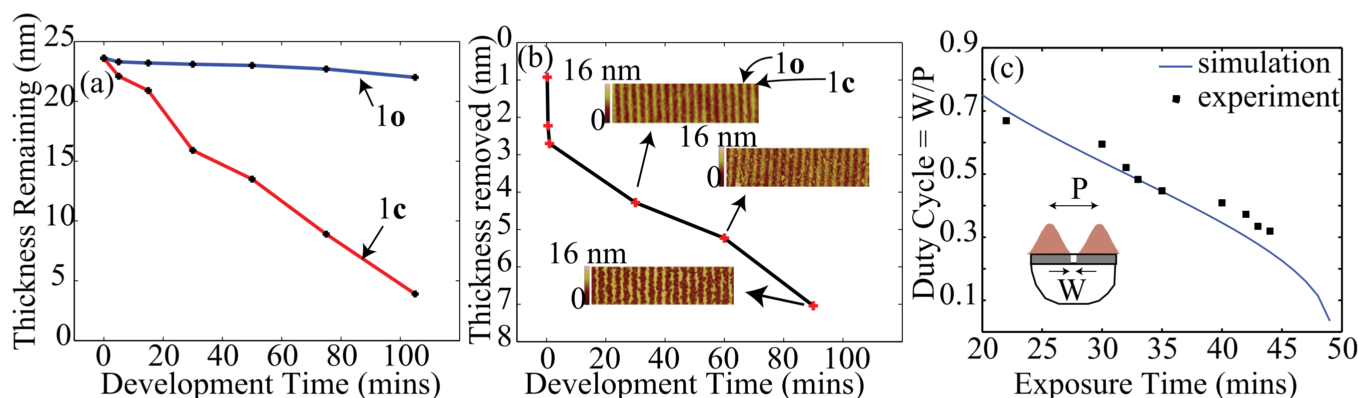

FIG. 2. (a) Macro-scale solubility of 1c and 1o in 100%(wt.) ethylene glycol. (b) Relative solubility of 1c vs 1o at the nanoscale (Inset: atomic-force micrographs of 3 development times). (c) Linewidth vs exposure time for a single exposure and development. The simulated curve is shown as a solid line while the experimental data are shown using solid squares. A sinusoidal illumination with period 526 nm was assumed.

In order to explain these observations, Density-Functional Theory (DFT) calculations were performed with the B3LYP functional and a standard 6-31G(d) basis set. The molecular geometries of both 1o and 1c were first optimized to a thermodynamic ground state and the electronic properties of both compounds then calculated using the Gaussian software interface. The ab initio calculated dipole moments for the open (1o) and closed (1c) forms are 5.65 D and 13.39 D, respectively. Details of this simulation are included in the supplementary material.[17] The higher dipole moment of 1c indicates that the closed-ring isomer is more polar and, therefore, comparatively more soluble in polar solvents. Again, this calculated trend agrees with the experimental observations that the closed-ring form, 1c, is more soluble compared to the open-ring form, 1o, in polar ethylene glycol.

Assuming an incident sinusoidal illumination, we can readily simulate the resulting feature size. In Fig. 1(c), this feature size as a fraction of the period of the illumination (526 nm in our experiments), i.e., the duty cycle, is plotted as a function of the exposure time using the solid black line. The experimentally measured values are shown using squares. Using the exposure threshold as the only fitting parameter, we can show that this simple model can accurately explain our experimental results. The smallest experimentally obtained duty cycle was 0.3, corresponding to a linewidth of ~158 nm or ~$\lambda/4$. More precise control of the exposure time should enable even smaller features. Note that as the exposure time is increased, the simulation indicates that feature size should be reduced significantly below the far-field diffraction limit.

Since the photochromic film can readily recover to its original state upon exposure to UV, it is straightforward to extend the idea to multiple exposures. This is, of course, required for creating dense patterns.[5] Here, we show feasibility of this approach by performing two exposures of the same standing wave, but with a ~45° rotation in between (Fig. 3). Each exposure was conducted on the Lloyd's-mirror interferometer, with a standing wave of period, 540 nm at $\lambda_2 = 647$ nm (incident intensity = 2.1 mW/cm^2) for 1 min.

After the first exposure, the sample was immersed in 100%(wt.) ethylene glycol for 30 min and exposed to short-wavelength UV lamp (UVGL-25, Analytika Jena AG) for 3 min to convert the molecules to the original closed-ring isomer 1c. The sample was then rotated approximately 45° relative to the optics, and a second exposure to the standing wave was performed. Again, the sample was immersed in 100%(wt.) ethylene glycol for 30 min. After each development, the sample was rinsed in deionized water and dried with N_2. The corresponding atomic-force micrograph resolves lines with spacing as small as ~260 nm or ~$\lambda/2.5$, which is less than half of the period of the standing wave. The significant line-edge roughness evident in Fig. 3 (right) is likely due to the partial oxidation of 1c under ambient condtions.[6] Improving the uniformity of the patterns requires that the exposure and development process be conducted under an inert atmosphere.

In conclusion, we introduced an approach to sub-diffraction-limited nanopatterning using low light intensities that exploits the solubility difference between photoswitchable

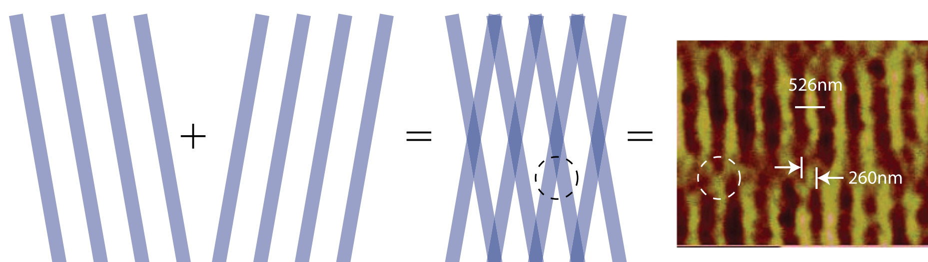

FIG. 3. Experimental demonstration of a double-exposure. Left: Schematic showing orientation of sample for double-exposure using POST. Right: Atomic-force micrograph of the resulting pattern. The atomic-force micrograph reveals the smallest spacing between the features as ~260 nm, which is approximately half the period of the illuminating standing wave.

This article is copyrighted as indicated in the abstract. Reuse of AIP content is subject to the terms at: http://scitation.aip.org/termsconditions. Downloaded to IP: 128.104.69.234 On: Thu, 31 Oct 2013 14:50:38

molecules and demonstrated the patterning of lines of width $\lambda/4$. We have also demonstrated isolated lines with resolvable features as small as $\lambda/2.5$, which is less than the far-field diffraction limit. This technique reduces the number of steps by avoiding an electrochemical oxidation as well as the requirement for a platinum working-electrode. Further optimization of the exposure and immersion parameters should lead to significantly reduced feature spacings. By extending the approach to 2D and even 3D, patterns of complex geometries may be readily patterned as well.

We thank Charles Fisher for assistance in the Utah Nanofabrication facility and Brian van Deveneer for assistance in the Surface Characterization Laboratory. P.C. acknowledges the NSF GRFP under Grant No. 0750758. P.C. acknowledges the University of Utah Nanotechnology Training Fellowship. R.M. acknowledges a NSF CAREER Award No. 1054899 and funding from the USTAR Initiative.

[1]X. Xie, Y. Liu, M. Zhang, J. Zhou, and K. S. Wong, Physica E **44**, 1109–1126 (2012).
[2]J. Leroy, A. Crunteanu, A. Bessaudou, F. Cosset, C. Champeaux, and J. C. Orlianges, Appl. Phys. Lett. **100**, 213507 (2012).
[3]D. W. Carr, L. Sekaric, and H. G. Craighead, J. Vac. Sci. Technol. B **16**, 3821 (1998).
[4]O. Wilhelmi, S. Reyntjens, C. Mitterbauer, L. Roussel, D. J. Stokes, and D. H. W. Hubert, Jpn. J. Appl. Phys. **47**(6), 5010–5014 (2008).
[5]N. Brimall, T. L. Andrew, R. V. Manthena, and R. Menon, Phys. Rev. Lett. **107**, 205501 (2011).
[6]P. Cantu, T. L. Andrew, R. Castagna, C. Bertarelli, and R. Menon, Appl. Phys. Lett. **100**, 183103 (2012).
[7]E. Abbé, Arch. Mikrosk. Anat. Entwichlungsmech. **9**, 413 (1873).
[8]L. Li, R. R. Gattass, E. Gershgoren, H. Hwang, and J. T. Fourkas, Science **324**(5929), 910–913 (2009).
[9]L. Li and J. T. Fourkas, Mater. Today **10**(6), 30 (2007).
[10]T. L. Andrew, H. Y. Tsai, and R. Menon, Science **324**(5929), 917–921 (2009).
[11]S. C. Laza, M. Polo, A. A. R. Neves, R. Cingolani, A. Camposeo, and D. Pisignano, Adv. Mater. **24**, 1304–1308 (2012).
[12]H.-Y. Tsai, S. W. Thomas III, and R. Menon, Opt. Express **18**(15), 16015 (2010).
[13]S. W. Hell, Science **316**, 1153 (2007).
[14]S. W. Hell, Phys. Lett. A **326**, 140 (2004).
[15]M. Switkes and M. Rothschild, J. Vac. Sci. Technol. B **19**, 2353 (2001).
[16]Y. Kim, T. J. Hellmuth, D. Sysoiev, F. Pauly, T. Pietsch, J. Wolf, A. Erbe, T. Huhn, U. Groth, U. E. Steiner *et al.*, Nano Lett. **12**, 3736–3742 (2012).
[17]See supplementary material at http://dx.doi.org/10.1063/1.4826925 for the modeling method, fabrication techniques, and dissolution characterization.

This article is copyrighted as indicated in the abstract. Reuse of AIP content is subject to the terms at: http://scitation.aip.org/termsconditions. Downloaded to IP: 128.104.69.234 On: Thu, 31 Oct 2013 14:50:38